Sci. Annals, Fac. Phys. & Mathem., Univ. Thessaloniki, 18, 267 (1978)

CONTRIBUTION TO THE STUDY OF THE SHEET-LIKE VOLCANIC BODIES EAST OF THE XANTHI PLUTONIC COMPLEX

by

G. CHRISTOFIDES*, G. ELEUTHERIADES** and K. SOLDATOS**

(Received 21.12.78)

Abstract: *Sheet-like volcanic bodies indruded, as sills and dykes, in the palaeogenic sediments E and NE of the Xanthi plutonic complex are described. The structure is more or less typical porphyritic. Plagioclase (An_{45}-An_{63}), amphiboles and pyroxenes occur both as phenocrysts and as microlites. The mineral constituents have optically and chemically been examined. From the data of six rocks chemical analyses it comes oat that these rocks belong to the calc-alkalic series. The magma originates very probably in the uppermost levels of the mantle and/or partly in the lower crust as indicated by the (τ) values.*

A. GEOLOGY

The area of the present study, covering about 30Km², is restricted between Mt. Mavropaedi (1070m) and the villages Filia, Ano Amaxades and Katsica (Fig. 1). In the sedimentary rocks of the above area which are in contact with the E and NE part of the Xanthi plutonic complex (Christofides, 1977), dark green to dark gray sheet-like volcanic bodies have been found (Fig. 2). Similar rocks concerning their occurrence and petrography were studied by Soldatos and Papadakis (1971) in the area NE of the Sunio village. These rocks were also mentioned by Dimitrov (1955) and considered as small apophyses of the Xanthi plutonic complex. It must be noted that similar sheet-like bodies occur also eastern and northeastern of the studied area.

The thickness of these sheet-like volcanic bodies varies greatly, from a few centimeters to 25 meters and they run for distances ranging

* Laboratory of Systematic Mineralogy and Petrography, University of Thessaloniki.

** Laboratory of Mineralogy and Petrology, University of Thessaloniki.

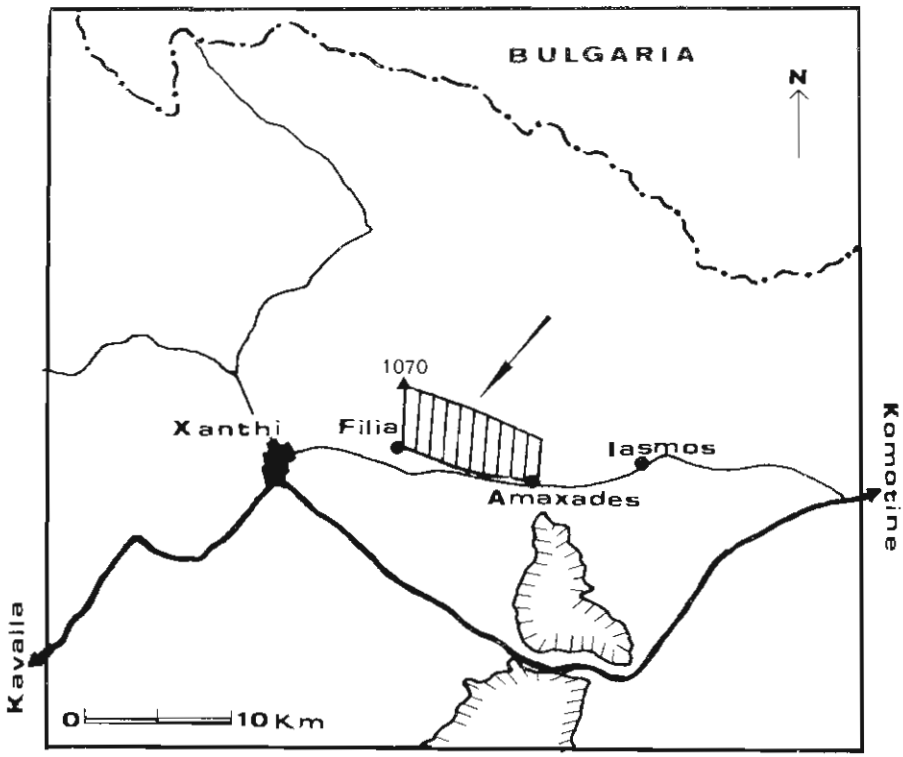

Fig. 1. Location of the studied area

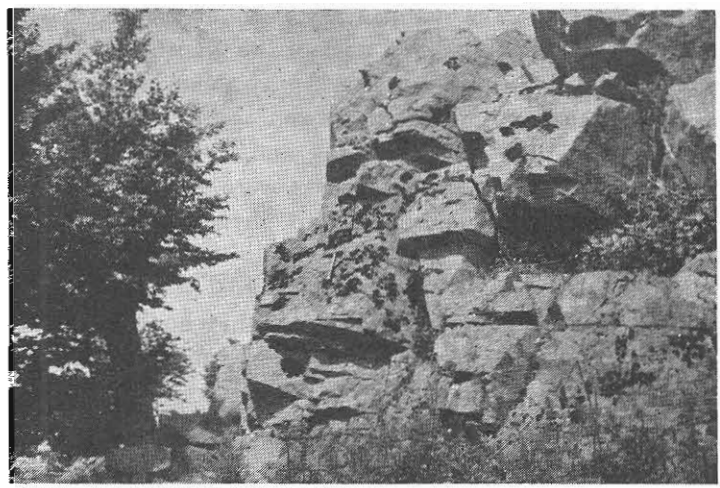

Fig. 2. Compact and unweathered sheet-like volcanic body S. of Mt. Mavropaedi (1070m).

from a few feet to about 500 meters. The bigger bodies are jointed with the main joint planes parallel to the contacts.

As in some instances these rocks are more resistant to weathering and erosion than their wall rocks, they project as a more prominent ridge. In other cases, however, they have been converted to soft soil as a result of an intensive weathering.

In general these rocks can be characterized as sills because most of them have been placed parallel to the bedding of the intruded sediments. Some of them, however, are intruded vertically and discordantly to the structures of the sediments and can be characterized as dykes. For convenience from now on these rocks will refer to as sills.

The sedimentary rocks through which the investigated rocks pass or into which intrude, belong to the Rhodope massif and are characterized as sandstones, claystones and arkoses of palaeogenic age. The strike of them is approximately E - W and the dip 45°-51° N.

The Rhodope massif (Osswald 1938, Neubauer 1957, Dimitrov 1955, 1959, Vergilov et al. 1963, Kockel and Walter 1965, Mercier 1966, Koukouzas 1972) occupies East Macedonia and Thrace and a part of South Bulgaria. According to Kockel and Walter (1965) it is built up by two series. The lower series, showing an effective thickness of about 10Km, is characterized by an ultrametamorphism and is restricted to the central and eastern Rhodope. This series is unconformably overlain by an upper series of mesozonal-metamorphosed rocks of 7-8Km thickness. In its lower part, as characteristic member, this series contains a horizon of leptinitic gneisses and in its upper part a sequence of marbles. Locally there is an uppermost sequence of schistose gneisses and calcareous schists, which is especially developed in the Bos Dag Mountains. The lowest parts of the series in the Rhodope massif is probably of precambrian age while the upper part of the series is of post-precambrian, very likely of palaeozoic age (pre-silurian).

B. PETROGRAPHY

In hand-specimens the colour of the sills examined is gray, gray-green to dark green. In appearence, however, their colour is somewhat lighter because of the weathering. One of the most striking features of these rocks are the amygdales with epidote, calcite and rarely quartz, formed mainly in altered samples. In addition throughout the length of

many of them their appearence is dominated by large prismatic phenocrystic hornblende up to 2cm long.

In general the investigated rocks are compact. This is due, very probably, to the escape of the gases from the magma before the relatively slow solidification of it. The relatively slow solidification of the magma is deduced from the matrix which is usually holocrystalline.

The femic-feldspar groundmass is holocrystalline, fine-to medium-grained. The structure is more or less typical porphyritic (Fig. 3) although some samples show a subdoleritic texture due to their coarser matrix.

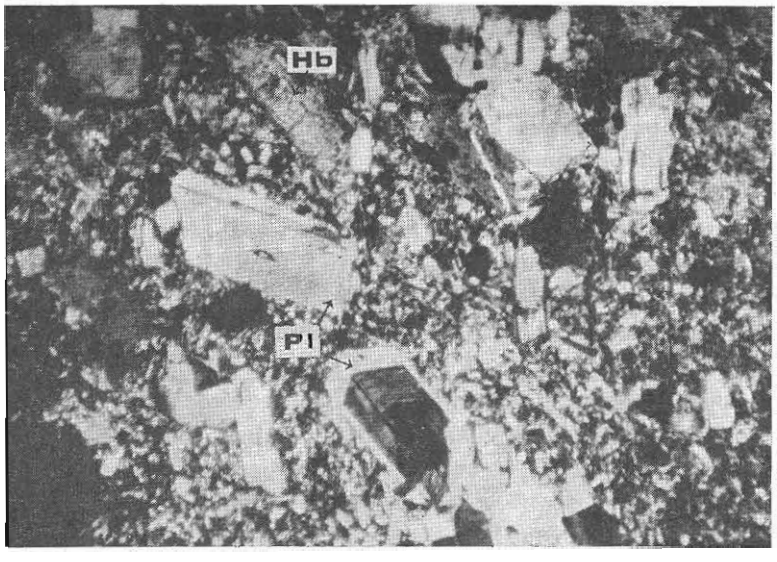

Fig. 3. Porphyritic structure. Pl=Plagioclase, Hb=Hornblende, ×32 N+.

At the margins of the sills the matrix is finer grained than the central parts. No contact metamorphism phenomena have been observed. The sediments have only slightly been baked.

The rocks examined have not been modally analysed because their matrix is too small to be identified. The amount of phenocrysts however, was roughly estimated and makes up to about 50 percent of the total rock volume. Phenocrystic plagioclase and hornblende are quantitatively the most important minerals. They are normally accompanied by clinopyroxene.

The rocks analysed were computed and classified using the RITTMANN norm (Rittmann, 1973) (Table I) and then plotted on the STRECKEISEN double-triangle (Streckeisen, 1967) (Fig. 4). As it can be seen from this diagram they cover the field of latitoandesite and andesite.

TABLE I

Rittmann norms of the analysed rocks

	1* (1F)	2 (273)	3 (2F)	4 (36)	5 (40Γ)	6 (50)	7 (7)
Quartz	—	1.0	—	—	—	—	2.2
Sanidine	10.0	18.4	11.2	5.8	6.9	4.6	3.4
Plagioclase	59.4	58.3	60.1	63.0	66.1	67.2	60.1
Normative anorthite	52%	47%	50%	48%	48%	46%	74%
Clinopyroxene	13.7	7.6	12.9	16.6	12.0	13.3	16.6
Orthopyroxene	7.5	11.8	5.1	2.0	0.7	2.3	14.6
Olivine	6.0	—	7.4	9.3	10.6	9.3	—
Magnetite	1.5	1.3	1.5	1.5	1.6	1.4	1.1
Ilmenite	1.4	1.1	1.4	1.2	1.5	1.3	1.5
Apatite	0.5	0.5	0.5	0.6	0.6	0.6	0.5
Colour index	30.6	22.2	28.7	31.2	27.0	28.2	34.3
Serial index (σ)	2.91	3.21	3.31	4.37	4.51	3.49	1.05
τ value	9.28	11.98	8.93	8.35	8.43	8.74	10.39

* 1-3 latitoandesites, 4-7 andesites

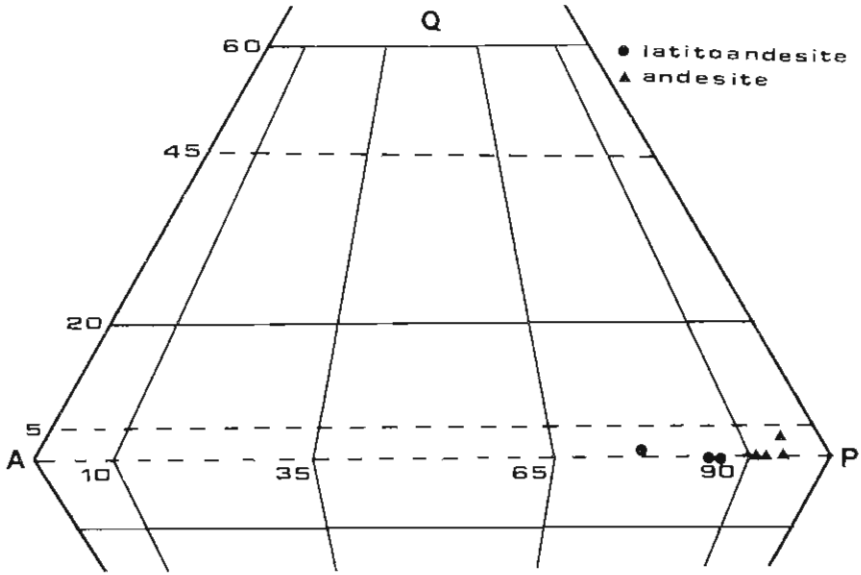

Fig. 4. Plot of calculated chemical analyses of the investigated rocks on the QAPF double-triangle according to the Rittmann norm.

The same field is also covered by latitobasalt and basalt respectively. The investigated rocks, however, could not be characterized as latitobasalts and basalts because their colour index (CI) is restricted between 22.2 and 34.3 while that of latitobasalts and basalts is >38 (38-70).

MINERALOGY

1. Plagioclase:

Plagioclase is the most abundant constituent mineral of the rocks examined and nearly the unique feldspar. They have been observed both as phenocrysts and as groundmass constituent. Plagioclase phenocrysts form idiomorphic crystals up to 3mm long.

Almost all the phenocrysts of plagioclase are zoned, either with normal or oscillatory zoning. The zoning of most phenocrysts follows the idiomorphic form of the crystals. The number of the zones is usually 10 to 15 although phenocrysts with more than 35 zones are not infrequent. The composition of the plagioclase phenocrysts, which was

determined on a U-stage, varies from An_{45} Ab_{55} to An_{65} Ab_{35}. These values agree in general with the anorthite composition determined by microprobe. The values of normative An are lower because they represent the mean composition of plagioclase. Twinning after Albite, Albite-Carlsbad and Carlsbad laws are the most common.

The core of some plagioclase phenocrysts or the whole crystal, is sometimes altered. Among the alteration products epidote and calcite have been observed. Inclusions of iron oxide, pyroxene and brownish dust are common.

The results of three chemical analyses (spot on the core), carried out by a microprobe analyser, are listed in Table II. In the same Table the atomic proportion of the elements on the basis of 32 (O) as well as the molecular proportion of An, Ab and Or are presented. Iron content is relatively high (0.75 wt%). This was also observed in plagioclase of the Almopia volcanic rocks (Eleutheriades, 1977).

Although there is a slight deficiency in alumina (Table III), the analysed plagioclases are characterised as normal plagioclases according to Wenk and Wilde (1973), because they are plotted very close to the line for the terrestrial normal plagioclases in the diagram $Al/(Al + Si)$ against $Ca/(Ca + Na + K)$.

The structural state of the plagioclase has been determined by the X-ray powder method of Smith and Gay (1958). Factor $\Gamma = 2\theta(131) + 2\theta(220) - 4\theta(1\bar{3}1)$ (in degrees) has been found to range between 1.05 and 1.15. From these values and the composition of the plagioclase it is deduced that the plagioclase is of the high temperature, disorded state.

2. Amphiboles:

Amphiboles are the most important femic constituents of the sills. Both green and brown hornblende have been identified. They occur as phenocrysts and in some samples with somewhat coarser groundmass as microlites. Green hornblende is generally more aboundant in the west part of the region examined, while the brown one predominates in the east part.

From microscopic studies of the amphiboles result that green hornblende is, at least for the most cases, an alteration product of primary pyroxenes (Fig. 5). This hornblende appears as single crystals or as aggregates of small prismatic crystals. Alternatively, brown hornblende which always forms single crystals never comes directly from pyroxenes.

TABLE II

Electron microprobe analyses of plagioclase

	(1)	(2)	(3)
SiO_2	53.04	53.27	51.79
TiO_2	0.15	——	——
Al_2O_3	28.47	28.38	29.34
FeO*	0.75	0.65	0.68
CaO	12.19	12.25	13.22
Na_2O	4.36	4.48	4.04
K_2O	0.12	0.15	0.12
Total	99.08	99.18	99.19
Numbers of ions on the basis of 32 oxygens			
Si	9.720	9.749	9.514
Ti	0.020	——	——
Al	6.150	6.124	6.354
Fe^{2+}	0.114	0.099	0.105
Ca	2.393	2.402	2.602
Na	1.549	1.590	1.437
K	0.027	0.035	0.029
Z	16.004	15.972	15.973
X	3.969	4.027	4.068
An	60.29	59.65	63.96
Ab	39.03	39.48	35.33
Or	0.68	0.87	0.71

* Total iron as Fe^{2+}. Iron is added in the Z group.

TABLE III

Calculated chemical analyses (molecular proportions) of plagioclase

						Excess or deficiency mol.%		Mol.
	SiO_2	Al_2O_3	CaO	Na_2O	K_2O	$\pm SiO_2$	$\pm Al_2O_3$	An%
(1)	882.68	279.28	217.37	70.34	1.27	+2.07	—3.47	60.28
(2)	886.50	278.40	218.44	72.28	1.59	+0.72	—5.00	59.65
(3)	861.87	287.82	235.73	65.18	1.27	—0.96	—4.99	63.95

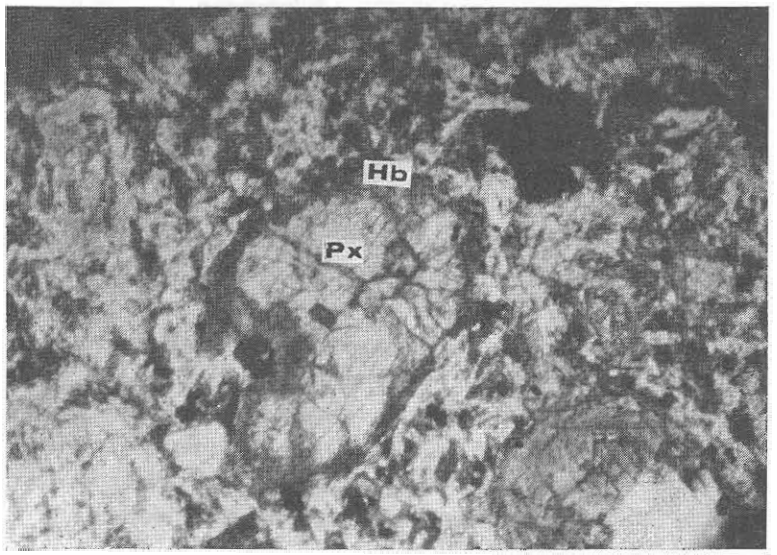

Fig. 5. Alteration of pyroxene (Px) to green hornblende (Hb). ×51 N—.

The two amphiboles are genetically related, as can be deduced by the fact that green hornblende is rimmed by brown hornblende (Fig. 6).

Both green and brown hornblende have strong pleochroism, the former being green to bluish green and the latter light brown to brown. The optic axial angles $2V\alpha$, determined on a U-stage, range in green and brown hornblende, from 76° to 78° and from 78° to 82° respectively.

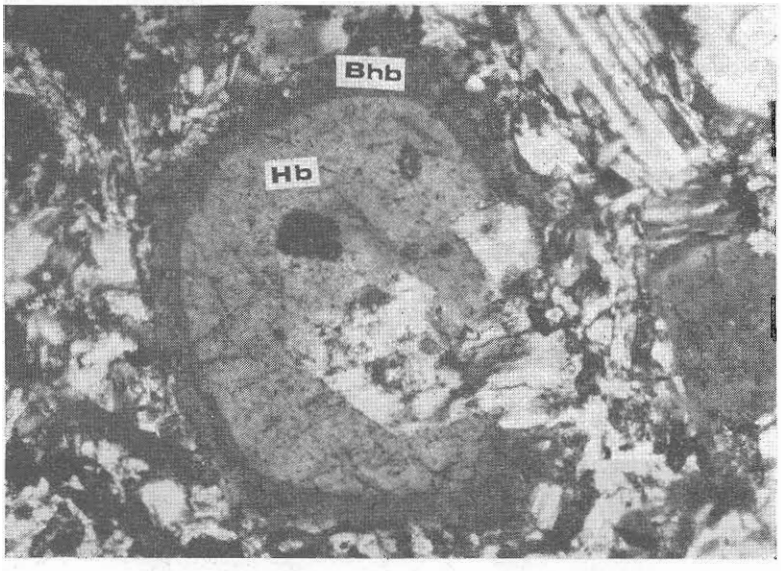

Fig. 6. Green hornblende (Hb) rimmed by brown hornblende (Bhb). $\times 121$ *N+.*

The extinction angle n_γ: c in brown hornblende is smaller (8°-15°) than that of the green one (17°-21°). Dispersion is in both cases r<v.

Brown hornblende exhibits, not infrequently, marginal resorption with dusty margins of fine opaque minerals. The fact that the dust of iron left from the hornblende is not strewn about indicates that much of the resorption took place after the intrusion of the magma.

The optical features of the brown hornblende agree in general with those of the so-called oxyhornblende. The relatively low Fe^{3+}/Fe^{2+} ratio (Table IV), however, does not allow the characterization of it as oxyhornblende.

In Table IV three chemical analyses of brown hornblende and one of green hornblende, carried out by a microprobe, are listed. (FeO was analysed by $KMnO_4$ method). Their atomic proportion on the basis of 23 (O) are also given in the same Table. Plot of Al^{IV} against (Na+K) of the analysed amphiboles on the respective diagram (Deer et al., 1963) shows that the green amphibole is of hornblende composition while the brown ones are of pargasitic composition (Fig. 7). The same samples are classified according to Leake (1968) as magnesio-hornblende and ferro-pargasite respectively.

TABLE IV

Electron microbrobe analyses of amphiboles

	1	2	3	4
SiO_2	39.97	39.30	41.00	48.18
TiO_2	2.79	2.82	3.47	1.23
Al_2O_3	13.95	14.77	12.65	5.61
Fe_2O_3	4.60	5.05	6.25	n.d.
FeO	7.57	6.68	7.03	16.60*
MnO	0.26	0.14	0.23	0.26
MgO	12.83	12.92	13.04	11.12
CaO	11.86	11.90	11.33	12.49
K_2O	1.10	1.01	1.00	0.38
Na_2O	2.71	1.92	2.59	0.47
Total	97.64	96.51	98.82	96.49

Numbers of ions on the basis of 23 oxygens

Si	5.903	5.835	5.988	7.246
Al^{IV}	2.097	2.165	2.012	0.754
Al^{VI}	0.332	0.421	0.166	0.241
Ti	0.310	0.315	0.381	0.139
Fe^{3+}	0.511	0.564	0.687	n.d.
Fe^{2+}	0.935	0.830	0.859	2.088*
Mn	0.033	0.018	0.028	0.033
Mg	2.824	2.859	2.838	2.493
Ca	1.877	1.893	1.773	2.013
Na	0.776	0.553	0.734	0.137
K	0.207	0.191	0.186	0.073
Z	8.000	8.000	8.000	8.000
Y	4.945	5.007	4.959	4.994
X	2.860	2.637	2.693	2.223
$\frac{Fe^{3+}}{Fe^{2+}}$	0.55	0.68	0.80	n.d.

* Total iron as Fe^{2+}.

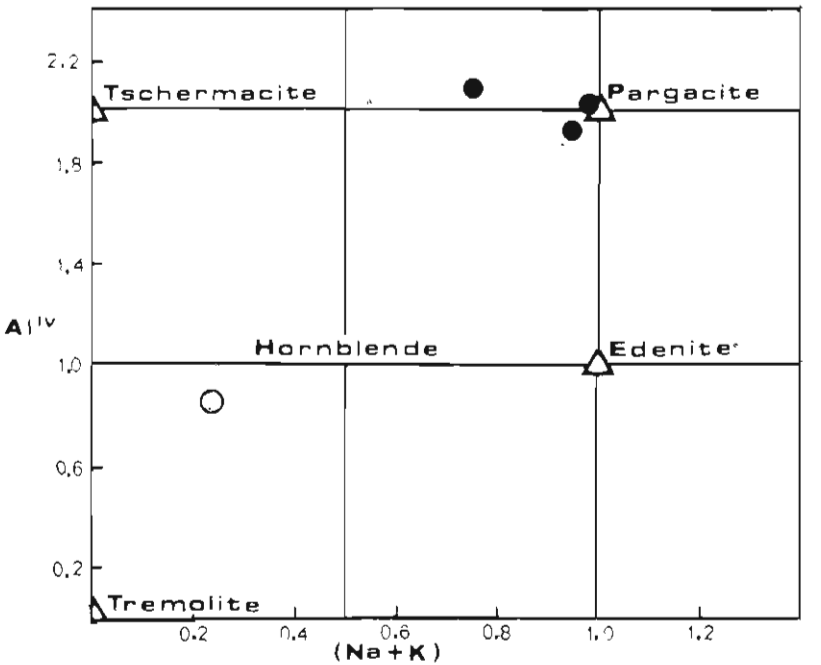

Fig. 7. The chemical variation of the analysed amphiboles expressed as the numbers of (Na, K) and Al^{IV} atoms per formula unit.
●=*brown hornblende,* ○=*green hornblende*

3. Pyroxenes:

Pyroxenes occur in most samples generally in small quantities. However, in the west part of the area investigated and particularly in Mt. Mavropaedi they are more abundant than hornblende which, as previously was mentioned, is the predominant ferromagnesian constituent of these rocks. Two generations of pyroxenes have been observed, as phenocrysts and as groundmass constituent. Orthopyroxenes have not been found in the samples examined.

In thin section, pyroxenes are colourless and form idiomorphic or rounded crystals. They are twinned on (100). Multitwinning is not uncommon. Zoning which is not infrequent throughout these rocks has also been observed. The optical axial angles $2V_\gamma$ determined on a U-stage, range between 52° and 54°. Dispersion of the optic axes is weak r>v. The extinction angle $n_\gamma : c$ varies from 40° to 43°.

Pyroxenes are more or less altered to a pale green amphibole (Fig. 5). The alteration, which begins around the periphery, extends very often to the whole crystal. In these cases pseudomorphs of hornblende after pyroxene are formed. Chlorite, epidote and sometimes carbonates are generally among the alteration products. Inclusions of opaque minerals are the most common ones.

From the data of three chemical analyses of pyroxene phenocrysts (Table V) and with the use of Di-Hd-En-Fs diagram (Poldervaart and Hess, 1951) the analysed pyroxenes are classified as salite.

4. Magnetite:

Fine-grained crystals of magnetite are present in most samples. Grains of it are not infrequently included in phenocrysts of ferromagnesian minerals and of feldspars. Secondary magnetite also occurs, especially as a by-product of the resorption of brown hornblende phenocrysts.

5. Apatite:

Its presence is relatively rare. It forms stout prismatic or rounded crystals up to 0.2mm long which are enclosed in amphiboles and rarely in pyroxenes. Needlelike crystals also occur in groundmass of high crystallinity.

6. Calcite:

It is a secondary mineral occurring in veins and in cavities as abnormal masses. Well-formed crystals were found in amygdales up to 6cm long, associated very often with epidote and sometimes with quartz.

The genesis of these amygdales is the result of a hydrothermal deposition. Calcite also occurs as a by-product of the other mineral constituents alteration.

7. Quartz:

It is also a secondary mineral, and as it was mentioned above, occurs in amygdales associated with calcite and epidote. Its undulatory extinction is characteristic.

Other accessory minerals of the studied rocks are secondary chlorite, pyrite, zircon, epidote and kaolinite.

TABLE V

Electron microprobe analyses of pyroxenes

	(1)	(2)	(3)
SiO_2	50.29	49.28	48.99
TiO_2	0.45	0.93	0.85
Al_2O_3	2.98	5.40	5.35
FeO*	13.01	6.76	6.85
MnO	0.43	0.27	0.20
MgO	9.31	14.24	13.98
CaO	23.95	21.91	22.22
Na_2O	0.55	0.43	0.58
Cr_2O_3	———	———	0.13
Total	100.97	99.22	99.15

Numbers of ions on the basis of 6 oxygens

Si	1.912	1.842	1.837
Al^{IV}	0.088	0.158	0.163
Al^{VI}	0.046	0.080	0.074
Ti	0.013	0.026	0.024
Fe^{2+}	0.414	0.211	0.215
Mn	0.014	0.009	0.006
Mg	0.527	0.793	0.781
Cr	———	———	0.004
Ca	0.976	0.878	0.893
Na	0.040	0.031	0.042
Z	2.000	2.000	2.000
Y	1.014	1.119	1.104
X	1.016	0.909	0.935
Wo	50.54	46.43	47.11
En	27.29	41.93	41.22
Fs	22.17	11.64	11.67

* Total iron as Fe^{2+}

TABLE VI

Chemical analyses and C.I.P.W. norms of the studied rocks

	1	2	3	4	5	6	7[1]
	(1F)	(273)	(2F)	(36)	(40Γ)	(50)	(7)
SiO_2	49.97	54.25	50.08	48.08	48.56	49.97	47.69
Al_2O_3	17.49	18.59	17.68	15.86	17.02	17.17	18.19
Fe_2O_3	1.90	2.72	2.12	3.43	4.06	3.03	3.71
FeO	8.00	5.28	7.60	5.94	5.62	5.73	6.64
MnO	0.17	0.15	0.16	0.17	0.16	0.17	0.19
MgO	6.01	3.99	5.87	6.16	5.78	6.40	5.12
CaO	9.54	7.72	9.20	8.92	8.33	9.86	12.27
Na_2O	2.73	3.37	2.95	3.33	3.54	3.71	1.25
K_2O	1.77	2.64	1.89	1.38	1.47	1.22	0.97
TiO_2	1.37	1.03	1.42	1.20	1.32	1.24	1.41
P_2O_5	0.22	0.24	0.23	0.30	0.28	0.30	0.22
L.O.I.[2]	1.16	0.42	0.98	4.90	3.50	1.36	2.09[3]
Total	100.33	100.40	100.18	99.67	99.64	100.16	99.75

Norms wt. %

Q		———	1.915	———	———	———	———	4.093
Or		10.459	15.600	11.168	8.155	8.687	7.209	5.732
Ab		23.101	28.516	24.962	28.178	29.954	30.164	10.577
An		30.241	27.801	29.418	24.252	26.209	26.593	41.157
Ne		———	———	———	———	———	0.666	———
Wo	Di	6.534	3.729	6.147	7.532	5.548	8.502	7.631
En	Di	3.601	2.205	3.475	4.940	3.779	5.652	4.622
Fs	Di	2.689	1.337	2.414	2.063	1.335	2.229	2.593
En	Hy	4.606	7.732	3.333	2.678	3.301	———	8.129
Fs	Hy	3.438	4.689	2.316	1.122	1.166	———	4.560
Fo	Ol	4.738	———	5.474	5.406	5.126	7.209	———
Fa	Ol	3.898	———	4.191	2.489	1.995	3.134	———
Mt		2.755	3.944	3.074	4.973	5.887	4.393	5.379
Il		2.602	1.956	2.697	2.279	2.507	2.355	2.678
Ap		0.510	0.556	0.533	0.695	0.649	0.695	0.510

1. Analysis from Soldatos and Papadakis (1971).
2. L.O.I.=Loss on ignition
3. H_2O+

C. PETROCHEMISTRY

In attempting to study petrochemically these sills, seven representative samples were chemically examined. The results of the analyses with the calculated C.I.P.W. norms are presented in Table VI. Their Niggli values and basis components as well as composite components Q, L, M and π, γ, μ values, were computed and are listed in Tables VII, VIII and IX.

The correlation of variations in the chemical constituents and values cited above, arrived at by the Niggli and Rittmann methods as well as by various diagrams, help us to reach to some conclusions concerning the chemism of the rocks examined.

On the diagram QLM (Fig. 8) the analysed rocks are plotted below the saturation line PF and cover the triangle PFR*. Projection points in this triangle may correspond to the mineral combinations pyroxene-feldspar-olivine or pyroxene-feldspar-feldspathoid. The normative composition of the plotted rocks agree with the first mineral combination.

TABLE VII

Niggli values of the analysed rocks

	si	al	fm	c	alk	ti	p	k	mg	$\frac{2alk}{al+alk}$	qz
1F	120.2	24.9	41.6	24.4	9.1	2.5	0.1	0.30	0.52	0.54	—16.2
273	148.0	29.8	34.3	22.5	13.4	2.1	0.2	0.34	0.47	0.62	— 5.6
2F	121.6	25.4	40.8	23.9	9.9	2.6	0.2	0.29	0.52	0.56	—18.0
36	120.6	23.5	42.2	23.9	10.4	2.3	0.3	0.22	0.55	0.61	—21.0
40Γ	122.1	25.2	41.3	22.5	11.0	2.5	0.3	0.22	0.52	0.61	—21.9
50	123.1	24.8	41.3	23.1	10.8	2.4	0.3	0.18	0.57	0.61	—20.1
(7)	114.0	25.8	38.4	31.5	4.3	2.6	1.0	0.33	0.47	0.29	— 3.0

* Sample (7) shows slightly different chemical behaviour from the rest ones as can be seen from the following diagrams, due probably to its relatively high CaO and low alkalies.

TABLE VIII

Basis components of the analysed rocks

	Ru	Cp	Kp	Ne	Cal	Cs	Fs	Fo	Fa	Q
1F	1.0	0.3	6.4	14.8	18.4	4.8	2.0	12.7	2.5	30.0
273	0.7	0.3	9.4	18.1	16.7	2.8	2.8	8.3	6.4	34.5
2F	1.0	0.3	6.7	16.2	17.8	4.6	2.2	12.3	9.1	29.8
36	0.9	0.6	5.1	18.8	15.4	5.7	3.8	13.4	7.5	28.8
40Γ	1.0	0.6	5.5	19.8	16.3	4.3	4.3	12.4	6.9	28.9
50	0.9	0.6	4.4	20.3	16.1	4.7	3.2	7.0	13.5	29.3
(7)	1.0	0.5	3.7	7.0	25.8	5.8	4.0	11.0	8.3	32.9

TABLE IX

Composite componets Q, L, M, and π, γ, μ values of the analysed rocks

	Q	M	L	π	γ	μ
1F	30.0	30.4	39.6	0.46	0.17	0.44
273	34.5	21.3	44.2	0.38	0.14	0.41
2F	29.8	29.5	40.7	0.44	0.16	0.44
36	28.8	31.9	39.3	0.39	0.19	0.44
40Γ	28.9	29.5	41.6	0.39	0.15	0.44
50	29.3	29.9	40.8	0.39	0.17	0.25
(7)	36.5	32.9	30.6	0.71	0.20	0.23

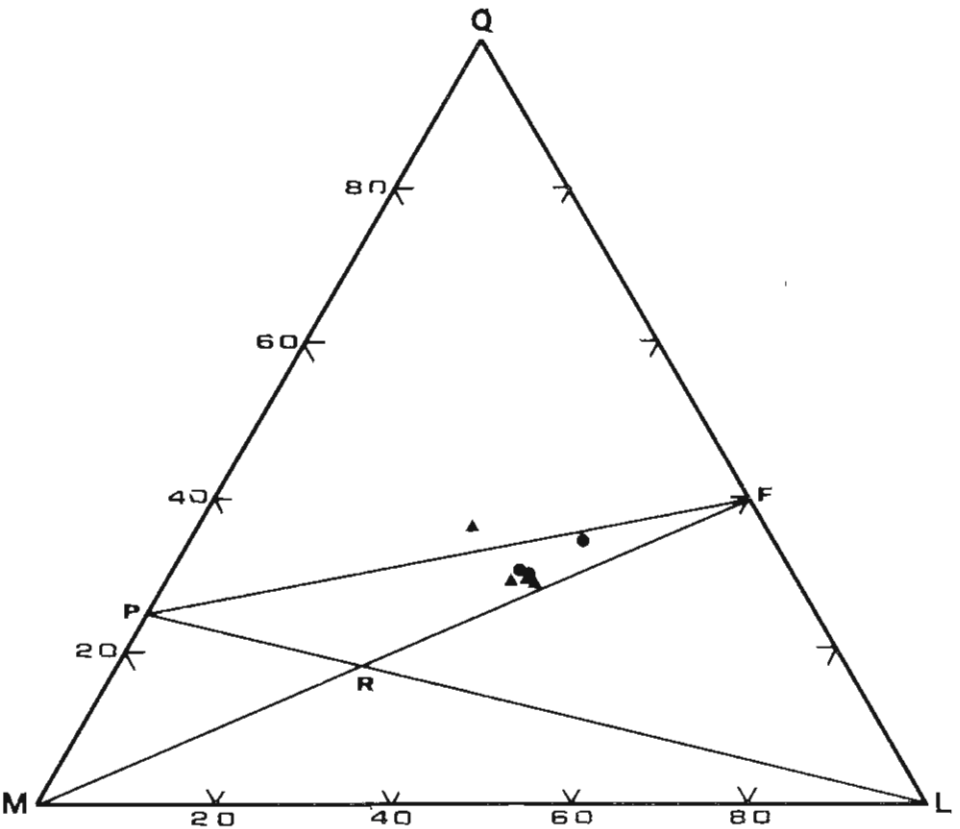

Fig. 8. Plot of the analysed rocks on the QLM - triangle. Symbols as in Fig. 4.

In the KNaCa-triangle (Fig. 9), which shows the quantitative relations of the Ca, Na, and K that are bound to Al, the values k and π are projected. From the projection points it is shown that the normative composition of the plagioclase is slightly lower than the composition found by optical and chemical methods.

From the MgFeCa-triangle (Fig. 10), which illustrates the quantitative relations of the Fe, Mg and Ca not bound with Al, it is evident that the ratio Mg : Fe is about 1 : 1.

Concerning the magma type it was found that the rocks examined belong, according to Burri and Niggli (1945, Burri 1964), to the gabbrodioritic and gabbroidal magmas of the calc-alkalic series. The calc-alkalic character of these rocks is also confirmed by the following:

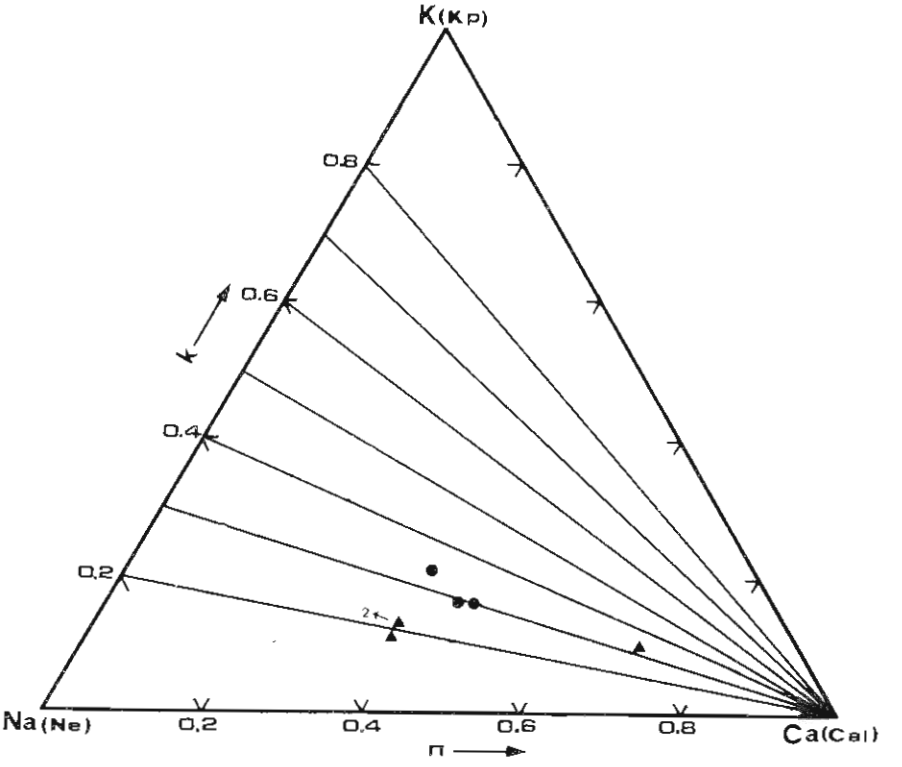

Fig. 9. Plot of the analysed rocks on the KNaCa - triangle. Symbols as in Fig. 4.

a) The AFM-diagram of figure 11 (Tilley, 1950). All the samples except (7) are plotted in the belt of composition variation of the calc-alkalic igneous rocks.

b) The FM-diagram ($F = FeO + Fe_2O_3$, $M = MgO$) of figure 12 (Tilley and Muir, 1967). The projection points are close to line 1 which corresponds to the calc-alkalic rocks series.

c) The serial index $\sigma = \frac{(Na_2O + K_2O)^2}{(SiO_2 - 43)}$ (Rittmann, 1957). According to the (σ) values the rocks belong to the calc-alkalic series. Two of them, however, are plotted in the transitional field (Fig. 13).

The magma type of the examined rocks is in agreement, as it can be seen from figure 14, with the magma type of the rhyolitic and ande-

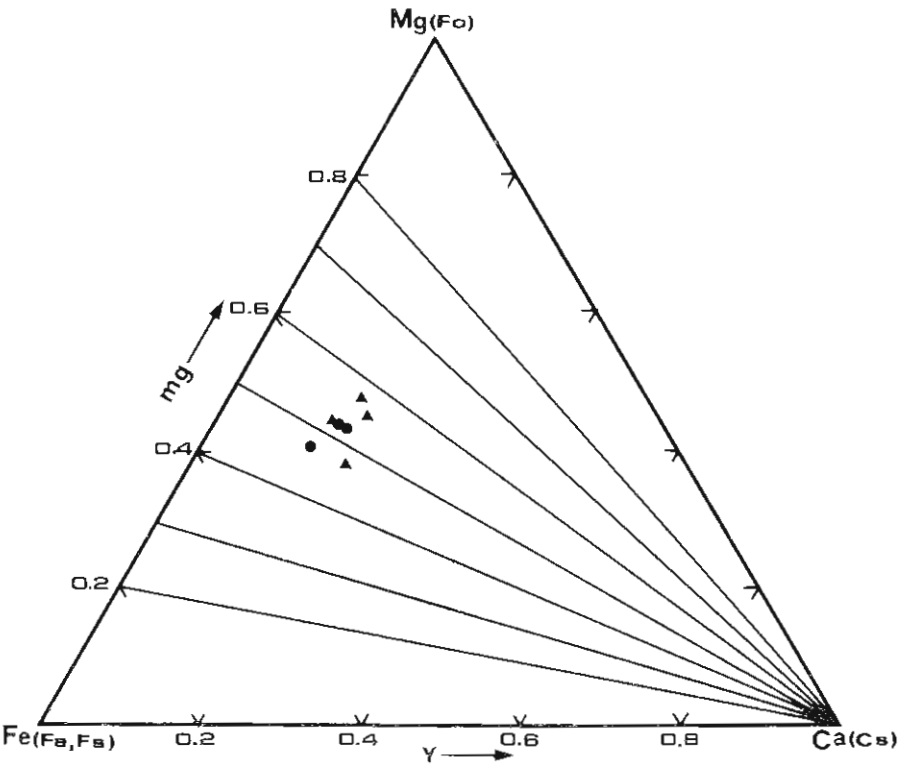

Fig. 10. Plot of the analysed rocks on the MgFeCa - triangle. Symbols as in Fig. 4.

sitic rocks of the so-called Rhodope province (Soldatos, 1961) as well as with that of the Xanthi plutonic complex (Christofides, 1977). Both the Rhodope province and the Xanthi plutonic complex are of calc-alkalic character.

The fact that similar rocks have also been found northern of the studied area and the fact that the analysed rocks occupy the low-si part of the variation diagram of the Rhodope province, could be considered as an indication that these rocks consist the more basic members of the Rhodope province.

As far as concern the origin of the magma of these rocks it is concluded from the (τ) values (Table I) (Gottini, 1967) that it originates very probably in the uppermost levels of the mantle and/or partly in the lower crust. Gottini has found that rocks with (τ) values lower than

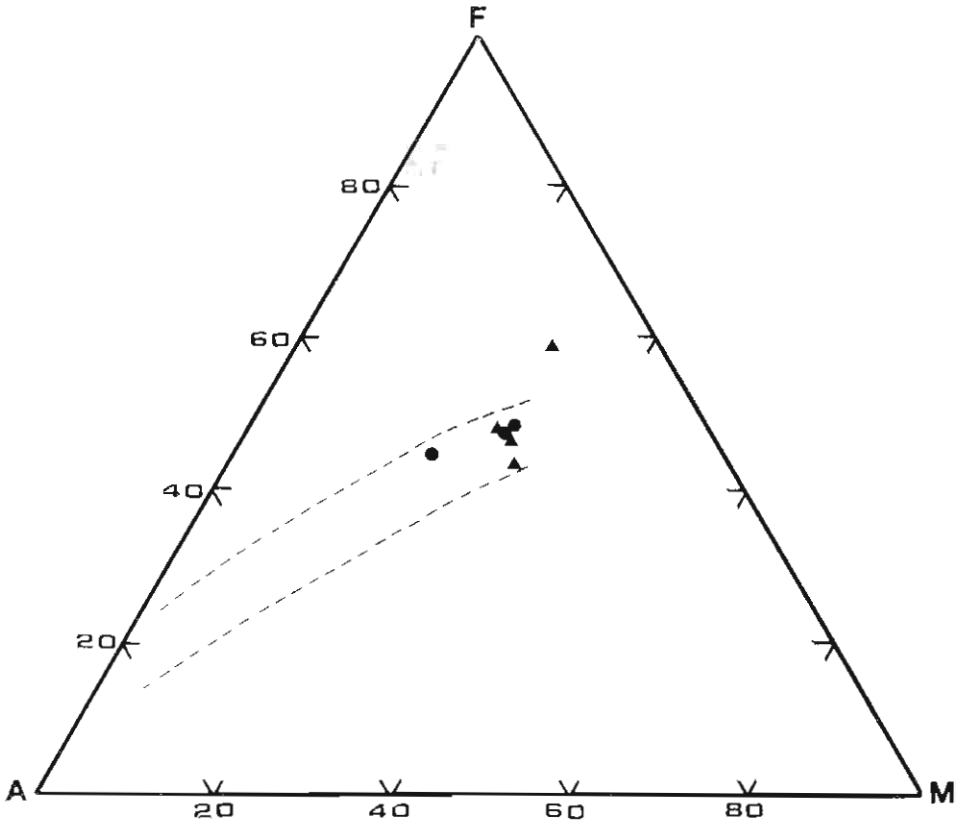

Fig. 11. Plot of the analysed rocks on the AFM-diagram. Dashed lines define the belt of composition variation of the calcalkakic igneous series. Symbols as in Fig. 4.

9 originate in the upper mantle, whereas those with (τ) values much more higher (>10) originate in the lower crust. Rocks with (τ) values between 9 and 10 originate in the boundary of the upper mantle and lower crust.

The presence of abundant hornblende crystals in these rocks means that the magma crystallization was proceeded, at least for a certain period, under high water pressure conditions. The widespread occurrence of early formed magnetite in most samples would also tend to indicate that the magma was generated under conditions of high water pressure. On the other hand the coexisting pyroxenes are considered as crystal-

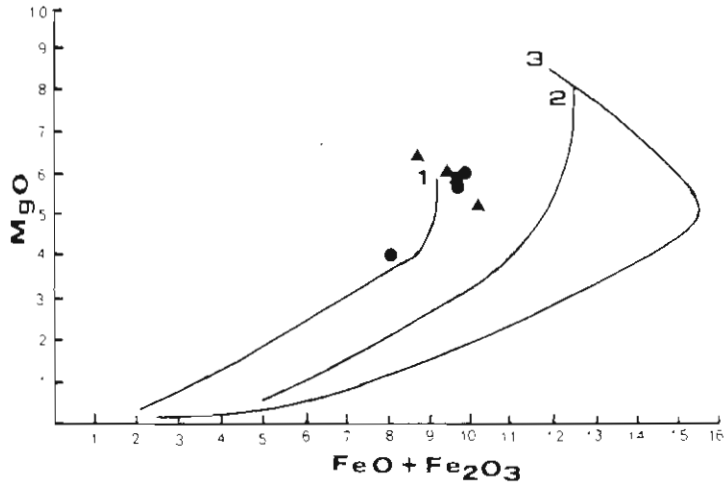

Fig. 12. Plot of the analysed rocks on the FM-diagram. 1: Calcalkalic series. 2: Alkalic series. 3: Tholeiitic series. Symbols as in Fig. 4.

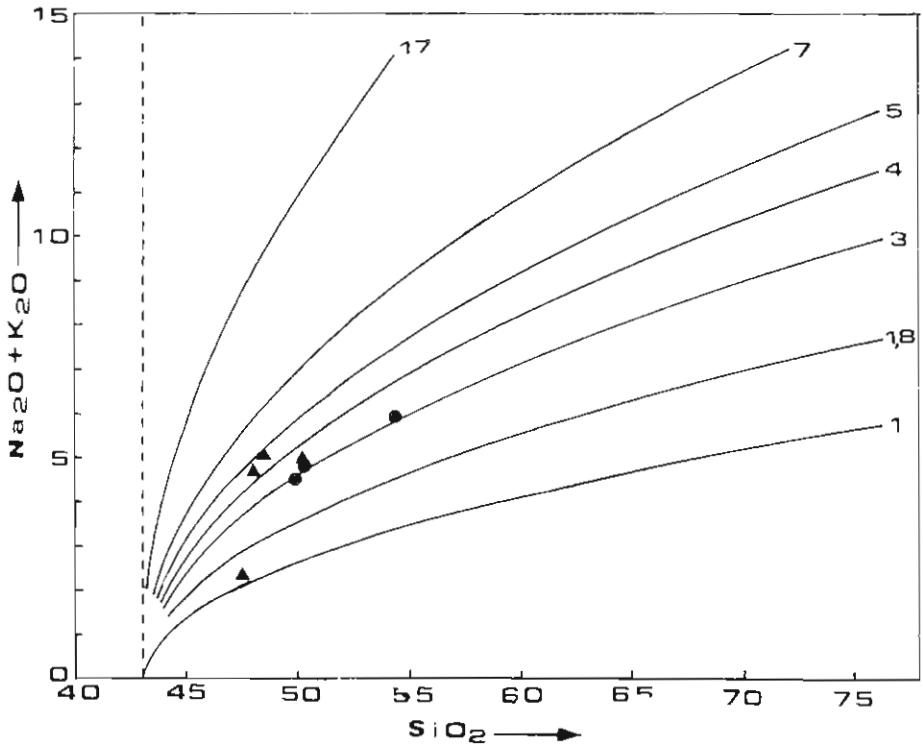

Fig. 13. The serial index (σ) of the analysed rocks, Symbols as in Fig. 4.

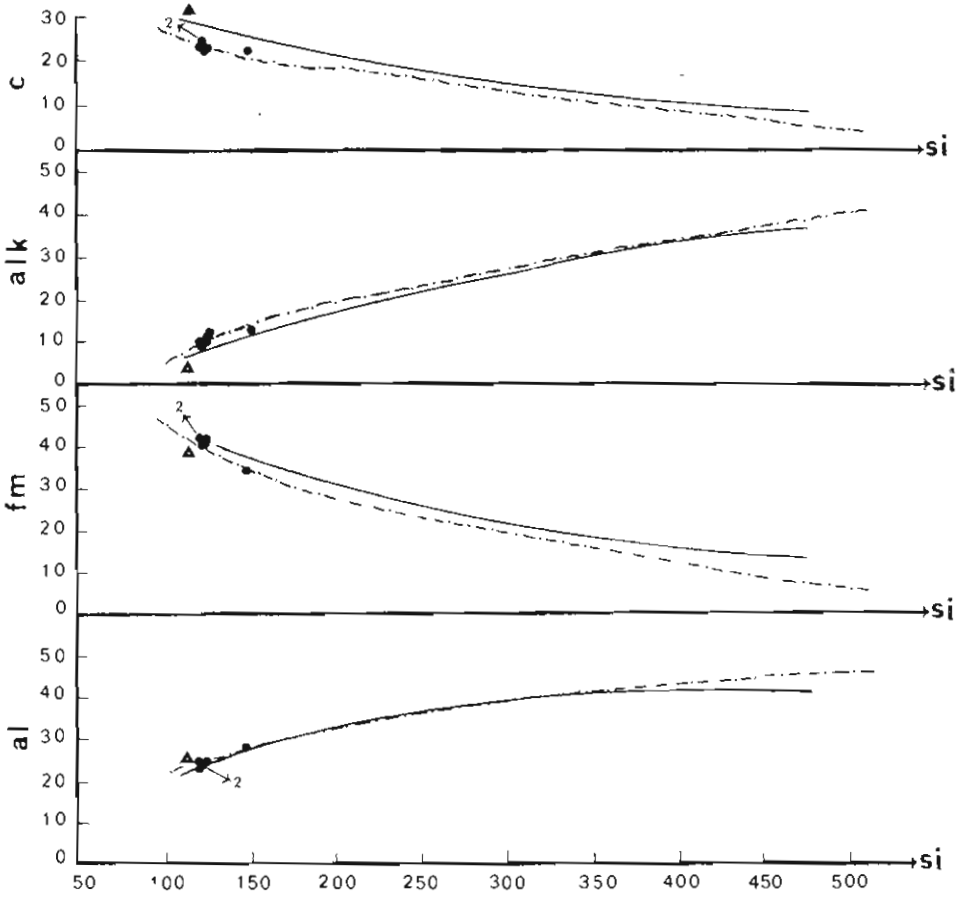

Fig. 14. Variation of al, fm, c and alk relotive to si for the analysed rocks in comparison with the calcalkalic volcanic rocks of the Rhodope province and the Xanthi plutonic complex.

——— *Rhodope province (Soldatos, 1961).*

····· *Xanthi plutonic complex (Christofides, 1977).*

● *Present study.*

Δ *Analysis taken from Soldatos and Papadakis (1971).*

lization products of a so-called «dry» magma. The coexistance of mineral facies such as hornblende and pyroxenes, which crystallize under different conditions means that these rocks display a mixed facies (Rittmann, 1973).

From the microscopic study of many thin sections it would be pos-

sible to accept the following stages for the crystallization process of the above mentioned mineral facies:

a) Crystallization of pyroxene in depth from a magma with moderate water pressure.
b) Increase of the pressure of the water remaining in the rest melt.
c) Separation of hornblende after the water pressure exceeds a certain value and beginning, under these «wet» conditions, of conversion of pyroxene marginally to amphibole.
d) Ascent of magma, escape of most gases and opacitization of amphibole.

ACKNOWLEDGEMENTS

The authors are grateful to Dr. J. V. P. Long of Cambridge University (Department of Mineralogy and Petrology) for his assistance in microprobe analyses, to Miss Marriner of Bedford College, London (Department of Geology) for her help in X.R.F. analyses, and to Mr. G. Xidakis of Leeds University (Earth Sciences Department) for performing part of the X.R.F. analyses. One of us (G. CH R.) gratefully acknowledges financial support from the Academy of Athens, Greece.

REFERENCES

Burri, C., (1964): Petrochemical calculations. Israel program for scientific translations. Jerusalem.

Christofides, G., (1977). Contribution to the study of the Xanthi plutonic complex. Ph. D. thesis, Thessaloniki University (in Greek).

Deer, W. A., Howie, R. A., and Zussman, J., (1963). Rock-forming minerals. Vol. 2, chain silicates. Longmans Press, London.

Dimitrov, Str., (1955). Stand und Aufgaben der Untersuchungen der magmatischen und metamorphen Komplexe Bulgariens. Izv. Akad. Nauk. SSSR, Ser geol. 1., 5-15.

» (1959). Kurze Übersicht der metamorphen Komplexe in Bulgarien. Freiberger Forschungsh., C57, 62-72.

Dimitrov, T., (1955). Bemerkungen über das Pluton bei Xanthi am Südrand der Rhodopenmasse (Bulg. mit Deut. zus). God. Sofijsk. Univ., Fac. Bio., Geol, and Geogr. Fak., t. XLIX, kn 2, Geol.

Eleutheriades, G., (1977). Contribution to the study of the volcanic rocks of South Almopia (Edessa). Ph. D. thesis, Thessalouiki University (in Greek).

Gottini, V., (1967). The TiO_2 frequency in volcanic rocks. Geol. Rund., 57, 930-935.
Kockel, F. and Walter, H.W., (1965). Die Strimonlinien als Grenze zwischen Serbo—Mazedonischem nnd Rila-Rhodope-Massiv in Ost-Mazedonia. Geol. Jb., 83, 575-602.
Koukouzas, C., (1972). Le chevauchement de Strymon dans la région de la frontiere grèco-bulgare. Z. Deutsch. Geol. Ges., 123, 343-347.
Leake, E. B., (1968). A catalog of analysed calciferons and subcalciferous amphiboles together with their nomenclature and associated minerals. Geol. Soc. Amer. Spec. paper, 98, 210 pp.
Mercier, J., (1966) Etude Geologique des zones internes des Hellénides en Macédoine centrale (Gréce). These, Univ. Paris.
Neubauer, W. H. (1957). Die Südgrenze der Rhodopen. Ein Beitrag znr stratigraphischen Anflösung der Kristallins anf der Halbinsel Chalkidike. Sitz. Ber. Österr. Akad. Wiss., math. natnrw. I, 166, 1-18.
Osswald, K., (1938). Geologische Geschichte von Griechisch-Nordmakedonien. Denkschr. Geol. Land. Griechenl., 3, Athen.
Poldervaart, A., and Hess, H. H., (1951). Pyroxenes in the crystallization of basaltic magmas. J. Geol., 59, 472-489.
Rittmann, A., (1957). On the serial character of igneous rocks. Egypt. J. Geol., 1, 23-48.
» (1973). Stable mineral assemhlages. Springer-Verlag, Berliu.
Smith, J. V., and Gay, P., (1958). The powder patterns and lattice parameters oi plagioclase feldspars. II. Min. Mag., 31, 744-762.
Soldatos, K., (1961). Die jungen Vulkanite der griechischen Rhodopen und ihre provinziellen Verhältnisse. Vulkaninstitut Immanuel Friedlaender. Zürich.
Soldatos, K., and Papadakis, A., (1971). Beitrag zur Kenntnis der östlich von Xanthi vulkanischen Gänge. Ann. Geol. Pays Hell., 23, 308-322 (In Greek).
Streckeisen, A., (1967). Classification and nomenclature of igneous rocks (Final report of an inquiry). N. Jh. Min. Abh., 107, 144-214, 215-240.
Tilley, C. E., (1950). Some aspects of magmatic evolution. Geol. Soc, London, Quart. J., 106, 37-61.
Tilley, C. E., and Muir, I. D., (1967). Tholeiite and tholeiitic series. Geol. Mag., 104, 337-343.
Vergilov, V., Kozuharov, D., Bojanov, I., Mavroudciev, B., and Kozuharova, E. (1963). Notes on the pre-paleozoic metamorphic complexes in the Rhodope Massiv. Bull. «Strassimir Dimitrov» Inst. Geol., 12, 187-211.
Wenk, H. R., and Wilde, W. R., (1973). Chemical anomalies of lunar plagioclase described by substitution vectors and their relation to optical and structural properties. Contr. Min. Petr., 41, 89-104.

ΠΕΡΙΛΗΨΗ

ΣΥΜΒΟΛΗ ΣΤΗ ΜΕΛΕΤΗ ΤΩΝ ΗΦΑΙΣΤΕΙΑΚΩΝ ΠΑΡΕΙΣΑΚΤΩΝ ΚΟΙΤΩΝ ΑΝΑΤΟΛΙΚΑ ΤΟΥ ΠΛΟΥΤΩΝΙΤΟΥ ΤΗΣ ΞΑΝΘΗΣ

ὑπὸ

Γ. ΧΡΙΣΤΟΦΙΔΗ*, Γ. ΕΛΕΥΘΕΡΙΑΔΗ** καὶ Κ. ΣΟΛΔΑΤΟΥ**

Ἐξετάζονται ἡφαιστειακὰ πετρώματα ποὺ μὲ μορφὴ κοιτῶν καὶ φλεβῶν διεισδύουν μέσα στὰ παλαιογενὴ ἱζήματα ποὺ βρίσκονται ἀνατολικὰ καὶ βορειοανατολικὰ τοῦ πλουτωνίτη τῆς Ξάνθης. Τὸ χρῶμα τῶν πετρωμάτων αὐτῶν κυμαίνεται ἀνάλογα μὲ τὸ βαθμὸ ἀποσαθρώσεως ἀπὸ ἀνοικτὸ γκριζοπράσινο μέχρι σκοτεινὸ γκριζοπράσινο. Ὁ ἱστός τους γενικὰ εἶναι ὁ τυπικὸς πορφυριτικὸς μὲ μερικὲς ἐξαιρέσεις δολεριτικῆς ἀναπτύξεως. Ὡς φαινοκρύσταλλοι συναντῶνται πλαγιόκλαστα, πυρόξενοι καὶ ἀμφίβολοι. Τὰ δύο πρῶτα ὀρυκτὰ παρουσιάζονται συχνὰ καὶ σὰν μικρόλιθοι, κάπως δὲ σπανιώτερα καὶ οἱ ἀμφίβολοι. Ἀπὸ τὴν ὀπτικὴ καὶ χημικὴ μελέτη τῶν ὀρυκτῶν συστατικῶν προκύπτει ὅτι τὰ πλαγιόκλαστα εἶναι συστάσεως ἀνδεσίνου-λαβραδορίου (An_{45}-An_{65}), οἱ ἀμφίβολοι συστάσεως παργασίτη καὶ κεροστίλβης καὶ οἱ πυρόξενοι σαλίτη. Ἀπὸ τὴν ἐπεξεργασία τῶν δεδομένων τῶν χημικῶν ἀναλύσεων ἕξι δειγμάτων πετρωμάτων προκύπτει ὅτι τὰ μελετηθέντα πετρώματα εἶναι λατιτοανδεσιτικῆς-ἀνδεσιτικῆς συστάσεως καὶ ὅτι ἀνήκουν στὴν ἀσβεσταλκαλικὴ σειρά. Ἀπὸ τὶς τιμὲς (τ) προκύπτει ὅτι τὸ μάγμα ποὺ τροφοδότησε τὰ παραπάνω πετρώματα κατὰ πᾶσα πιθανότητα προέρχεται ἀπὸ τήξη ὑλικοῦ τοῦ ἀνώτατου μανδύα μερικῶς δὲ καὶ τοῦ κατώτερου φλοιοῦ.

* Ἐργαστήριο Συστηματικῆς Ὀρυκτολογίας καὶ Πετρογραφίας τοῦ Παν/μίου Θεσσαλονίκης.

** Ἐργαστήριο Ὀρυκτολογίας - Πετρολογίας τοῦ Παν/μίου Θεσσαλονίκης.